



HAL
open science

Towards phonetic interpretability in deep learning applied to voice comparison

Emmanuel Ferragne, Cédric Gendrot, Thomas Pellegrini

► **To cite this version:**

Emmanuel Ferragne, Cédric Gendrot, Thomas Pellegrini. Towards phonetic interpretability in deep learning applied to voice comparison. ICPHS, Aug 2019, Melbourne, Australia. pp.ISBN 978-0-646-80069-1. halshs-02412948

HAL Id: halshs-02412948

<https://shs.hal.science/halshs-02412948>

Submitted on 16 Dec 2019

HAL is a multi-disciplinary open access archive for the deposit and dissemination of scientific research documents, whether they are published or not. The documents may come from teaching and research institutions in France or abroad, or from public or private research centers.

L'archive ouverte pluridisciplinaire **HAL**, est destinée au dépôt et à la diffusion de documents scientifiques de niveau recherche, publiés ou non, émanant des établissements d'enseignement et de recherche français ou étrangers, des laboratoires publics ou privés.

TOWARDS PHONETIC INTERPRETABILITY IN DEEP LEARNING APPLIED TO VOICE COMPARISON

Emmanuel Ferragne¹, Cédric Gendrot¹, Thomas Pellegrini²

¹Laboratoire de Phonétique et Phonologie (UMR7018, CNRS - Sorbonne Nouvelle)

²Institut de Recherche en Informatique de Toulouse (UMR5505, CNRS - Université de Toulouse)
emmanuel.ferragne@univ-paris-diderot.fr

ABSTRACT

A deep convolutional neural network was trained to classify 45 speakers based on spectrograms of their productions of the French vowel / \tilde{a} /. Although the model achieved fairly high accuracy – over 85 % – our primary focus here was phonetic interpretability rather than sheer performance. In order to better understand what kind of representations were learned by the model, i) several versions of the model were trained and tested with low-pass filtered spectrograms with a varying cut-off frequency and ii) classification was also performed with masked frequency bands. The resulting decline in accuracy was utilized to spot relevant frequencies for speaker classification and voice comparison, and to produce phonetically interpretable visualizations.

Keywords: voice comparison, deep learning, forensic phonetics, vowels.

1. INTRODUCTION

Ever since the sound spectrograph was invented in the 1940s [9], phoneticians have mostly relied on visualizations to identify the relevant parameters (formants, VOT, etc.) to describe phonetic entities (vowels, voicing, etc.). The advent of deep learning around 2010 has led to a situation where very powerful tools are now available to carry out this task automatically. A well-known advantage of deep neural networks (DNN) over more conventional machine learning algorithms is that they can extract features from the raw data without the need for a human expert to explicitly provide them to the model [5]. In other words, after 70 years or so of visual identification of acoustic cues to account for phonetic phenomena, DNNs could now potentially take over from human experts. On the downside, DNNs have earned a bad reputation because of their lack of transparency. We would like to show one way to overcome this difficulty with preliminary results we obtained in the field of forensic voice comparison.

In speech processing, DNNs have been successfully applied to acoustic modelling at phone level for speech recognition [7] and language identification [10], for instance. In speaker recognition, DNNs were efficient in an indirect manner: instead of being used as classifiers, they were used as feature extractors, with so-called bottleneck features [11] and embeddings [19]. In the current work, we performed speaker identification on a small speech dataset comprised of occurrences of one vowel. Thus, our work is closer to voice comparison rather than speaker identification, which would involve thousands of speakers and longer speech excerpts. DNNs, namely multi-layer perceptrons [13] and convolutional neural networks (CNNs) [16], have been shown to capture high-level phonetic properties when trained as phoneme recognizers. These studies highlighted that neuron units and convolution filters become selective to phonetic features such as manner and place of articulation.

We ran three experiments with a deep CNN and interpreted the output of our models in terms frequency bands located in the broadband spectrogram that phoneticians are most familiar with. In the first experiment the model classified 45 speakers based on their production of the French vowel / \tilde{a} /. In the second experiment the same model was retrained and tested with low-pass filtered tokens with various cutoff frequencies. In the third experiment, occlusion sensitivity was performed: we observed how the masking of certain frequency bands affected the model's performance. The vowel / \tilde{a} / was used because preliminary trials with other vowels from the same corpus showed that / \tilde{a} / yielded the highest speaker classification rates, which agrees well with the consistent finding in the literature that nasals, and especially nasal vowels [1], tend to contain more speaker-specific information than other segments.

2. SPEECH MATERIAL

The vowels used for classification were extracted from the ESTER Corpus [3], which is a collection of recorded journalistic radio broadcast generally considered as prepared rather than read or spontaneous speech [4]. *France Inter*, *France Info* and *Radio France International* constitute the three sources for our extractions. We used the phonetic alignment provided with the corpus by the IRISA (*Institut de Recherche en Informatique et Systèmes Aléatoires*) through the AFCP (*Association Francophone de la Communication Parlée*) website (http://www.afcp-parole.org/camp_eval_systemes_transcription/).

Automatic alignment was used to extract vowels with a rectangular window shape and without their phonetic context, the latter being neither controlled nor provided to the network for the discrimination.

3. SPECTROGRAMS

Phoneticians are used to reading broadband spectrograms. In the Praat program [2], default settings are 5-ms analysis frames and 2-ms hop size. Based on these values, we chose to use 5.0625 ms frames and 0.5 ms hop size to get a 90 % overlap between neighboring frames. With a 16 kHz sampling rate, these corresponded to frames of 81 samples. An odd number of samples allows to perform zero-phase windowing, which guarantees that the signal portions used to compute the Fast Fourier Transform (FFT) are as symmetric as possible in order to get pure real-valued spectra [18]. The speech segments were element-wise multiplied by a Hamming window and padded to obtain 512-sample segments on which FFT was computed. No pre-emphasis was applied since it increases the amplitude of high frequencies and decreases the amplitude of lower bands and, thus, changes the auditory perception when resynthesizing back to time domain. We avoided this artifact because we are planning perceptual experiments in the project. Finally, the dynamic range was set to 70 dB to prevent the CNN from identifying speakers based on dynamic instead of spectral cues. Other values were tested by resynthesizing several signals, and the 70 dB value was the one that least impacted the auditory perception of the speakers. Vowels whose duration was greater than 250 ms were left out; the shortest vowels were 30 ms long. Spectrograms of vowels shorter than 250 ms were padded with zeros in order for all spectrograms to have equal width. They were then converted to 8-bit grayscale images and resized to 224×224 pixels, where a pixel was equal to 1.15 ms in the time dimension and 35.71 Hz in terms of frequency. Con-

version to 8 bits was performed so that GPU memory would handle mini-batches of sufficient size for learning to take place.

4. MODEL

We used VGG16 [17], a well-known deep convolutional neural network that has become a reference in image recognition. VGG16 and variants called "VGGish" models [6] have been widely used in audio-related tasks for their simplicity and good performance, as in [14] for large-scale speaker identification. In our experiments, the model was re-trained from scratch with randomly initialized weights. All models were trained using an NVIDIA GTX 1080 GPU with the Adam optimizer [8], with a gradient decay factor of 0.900, and a squared gradient decay factor of 0.999. The initial learn rate was 0.0001 and the mini-batches contained 56 spectrograms.

5. EXPERIMENTS

The smallest number of / \tilde{a} / tokens produced by one speaker was 334; so 334 occurrences were randomly picked from the remaining 44 speakers, yielding a final dataset of 15,030 spectrograms. It was randomly split into a training, a validation, and a test set containing 10,530 (70 %), 1,485 (10 %), and 3,015 (20 %) tokens, respectively.

5.1. Speaker classification

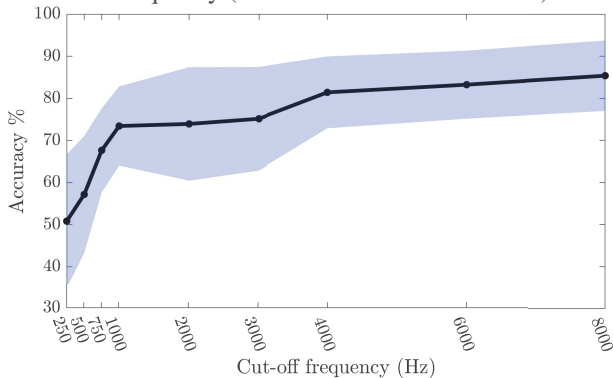
In this first experiment, speaker classification was carried out. The stopping criterion was reached after 8 epochs. The average accuracy of the model on the test set reached 85.37 % with individual scores ranging from 59.70 to 98.51 %. The mean score was 83.88 % for the 10 women and 85.80 % for the 35 men; the difference between men and women failed to reach statistical significance according to a Mann-Whitney U test ($p = 0.32$). While such a high classification rate constitutes an interesting finding in itself, it is quite frustrating for phoneticians because at this stage we have no means of knowing what representations the model has learned, and the small number of misclassified items does not quite lend itself to fruitful phonetic interpretation. To illustrate this point, among the 990 possible pairwise confusions, 235 contain non zero values; and among them, 194 are constituted of one or two misclassified tokens.

5.2. Low-pass filtered speech

The spectrograms used in Section 5.1 were cropped to obtain seven different versions of the original

dataset with maximal frequencies ranging from 250 to 6,000 Hz. The impact of cutoff frequency on model accuracy is shown in Fig. 1 (the results for the unaltered spectrograms were added for the sake of completeness). Fig. 1 shows a steep increase in accuracy between 250 and 1,000 Hz; then scores rise much more slowly from 1,000 Hz upwards.

Figure 1: CNN accuracy depending on low-pass cutoff frequency (mean and standard deviation).



The lowest accuracy score, 50.85 % obtained with a cut-off frequency of 250 Hz, was significantly above chance ($\chi^2 = 38479$ $p < 0.001$). Mid-p-value McNemar tests were conducted to check if improvements in accuracy from one model to the next were statistically significant. Each of the models with cut-off frequencies from 500 to 1,000 Hz shows a highly significant improvement over the model with the next lower cut-off frequency. The model with a cut-off at 2,000 Hz shows no significant improvement compared to the model with a cut-off at 1,000 Hz ($p = 0.580$). The 3,000 Hz model did not perform better than the 2,000 Hz ($p = 0.151$) or the 1,000 Hz model ($p = 0.074$). Then all remaining models improved on the preceding one, although the increased accuracy from 4,000 to 6,000 Hz was only marginally significant ($p = 0.012$).

A legitimate question here is whether speakers get consistent relative accuracy scores across all cut-off frequencies. In order to test this possibility, for each frequency, speakers were ranked according to their score and Kendall’s concordance coefficient was computed. The outcome was not statistically significant ($W = 0.11$ $\chi^2 = 43.39$ $df = 44$ $p = 0.50$), which supports the view that relative accuracy scores among speakers are inconsistent from one frequency step to the next.

5.3. Occlusion sensitivity

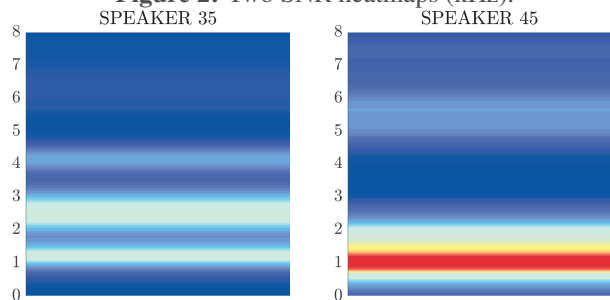
The model trained in Section 5.1 was used here. The test phase was different however: test spectrograms were modified by means of a mask (an array of zeros) occluding 15 contiguous pixels (≈ 536 Hz) in

the frequency dimension over the whole duration of the vowel. For each vowel, the position of the mask was moved iteratively by one pixel along the vertical axis, each time generating a new test image. The initial position of the mask only occluded the lowest pixel row of the spectrogram, and the final position was reached when only the topmost pixel row in the spectrogram was affected. The process yielded 252 new spectrograms for each of the 3,015 (67 test vowels \times 45 speakers) that were classified by the model.

At the end of the experiment, the 67 individual test spectrograms were converted to heatmaps where the color of a frequency band reflected the probability that the vowel belonged to its true speaker class when this frequency band had been occluded. In order to determine which frequency bands were typical of a given speaker, the mean and standard deviation of each speaker’s 67 heatmaps were computed, and a signal to noise ratio (SNR) was obtained by computing the pixel-wise ratio of the mean heatmap to the standard deviation heatmap for each speaker. The intensity values of the SNR heatmaps were rescaled to the interval ranging from the smallest to the highest value found in the whole dataset.

Fig. 2 shows two SNR heatmaps. The heatmap in the left panel, showing the output of the occlusion technique with the test vowels of Speaker 35, happens to contain the lowest SNR value in our data and therefore exemplifies the darkest shade of blue (slightly above 5 kHz). The picture to the right of Fig. 2 illustrates the highest SNR value (around 1 kHz) in our dataset, which is represented by the darkest type of red in our colormap.

Figure 2: Two SNR heatmaps (kHz).

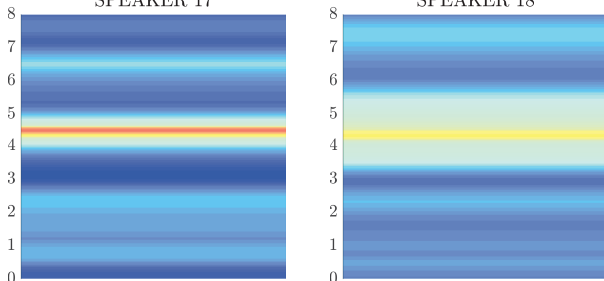


The salient red stripe shows that when this region in Speaker 45’s spectrograms is hidden from the model, the probability that Speaker 45 is correctly classified drops abruptly and the resulting performance deterioration is very consistent across all 67 test spectrograms for this speaker. In contrast, in the left panel of Fig. 2, though critical regions emerged for Speaker 35 (slightly above 1 kHz and between 2 and 3 kHz), they are not as strong as what was found for Speaker 45, hence their green to yellow color.

5.4. Linking classification, filtering and occlusion

While Speakers 35 and 45 have remarkable SNR heatmaps, containing either the minimal or maximal value computed over all speakers, their results in Section 5.1 and Section 5.2 are not markedly distinct. In the 1st experiment their accuracy scores lie between the 1st and 3rd quartile. Their accuracy curves in the 2nd experiment exhibit some differences: Speaker 35 displays a steep accuracy increase from 41.79 % (250 Hz) to 94.03 % (3,000 Hz) while Speaker 45's curve rises more slowly from 64.18 % to 88.06 % over the same frequency interval. The link between classification accuracy and what SNR heatmaps show is not straightforward. After computing distances between heatmaps and converting the confusion matrix from experiment 1 to distances, the correlation between the two matrices was rather weak: $r = 0.187$ (though highly significant: $p < 0.001$ according to a Mantel test with 100,000 permutations). To what extent the visual similarity between two heatmaps reflects confusability between two speakers is further exemplified by Fig. 3: the heatmaps look similar and the speakers show confusions in all the models. However, this pair is not the one that exhibits the highest confusion rates; a visual analysis of the two SNR heatmaps is therefore not good indicator of confusability.

Figure 3: Two similar SNR heatmaps (kHz).
SPEAKER 17 SPEAKER 18



A careful visual inspection of all SNR heatmaps suggests that at least 35 of the 45 heatmaps display a relatively strong frequency band around 1 kHz, like both heatmaps in Fig. 2, which points to the importance of this region to characterize a speaker's voice.

6. DISCUSSION AND CONCLUSION

DNNs have often been regarded as blackboxes because of the opaqueness of their inner mechanisms, but efforts have been made in recent years to provide experts in different fields with easily interpretable visualizations of what DNNs learn. Most of these techniques were invented in the context of image recognition and computer vision, and we tried to adapt one of them to spectrograms. As far as we can

tell, the method we used here, inspired by [21], as well as the localization of discriminative regions in [22] or saliency maps in [15] (the latter in the field of audio signal processing) can all be successfully transferred to the study of phonetics.

Our heatmaps constitute data-driven representations of potentially critical spectral regions that are typical of a given speaker's voice. We devised a method that combines information about how critical a spectral region is and how consistent this region is across several spectrograms of a speaker. A thorough visual analysis of the SNR heatmaps reveals two important features: first, not all speakers display such critical and reliable frequency bands to the same extent, and second, whenever critical bands are present, they can be found in different regions from one speaker to the next although the 1 kHz region is quite consistently present for most speakers. More research is needed to explore the full potential of our SNR heatmaps especially because, as we have shown, two very similar images do not necessarily correlate with high reciprocal confusability. Intuitively, an interesting connection may exist between a heatmap and the concept of distinctiveness in perceptual voice recognition [20], if we go so far as to equate high spectral saliency and low within speaker-variation to distinctiveness.

Spectrograms of the French vowel / \tilde{a} / were fed to a CNN to perform speaker classification based on a corpus of 45 speakers. While accuracy rates were satisfactory, low-pass filtering with varying cut-off frequencies and occlusion sensitivity were used to discover what features the model had learned. A notable finding was that even when the model had very little information (spectral content only up to 250 Hz) it performed well above chance. Another key finding made possible by our new SNR heatmaps is that many speakers displayed a critical region – a frequency band that, when occluded, led the speaker to be misclassified – around 1 kHz. While SNR heatmaps constitute a promising approach to understanding what DNNs learn, they have yet to be validated with perceptual experiments, which is our next logical step in the project. On the epistemological level, we hope that this study exemplifies how the (statistical) acoustic-phonetic and the automatic approaches to forensic voice comparison [12] can potentially reinforce each other.

7. ACKNOWLEDGEMENTS

This work was supported by the Agence Nationale de la Recherche projects VOXCRIM (ANR-17-CE39-0016) & LUDAU (ANR-18-CE23-0005-01).

8. REFERENCES

- [1] Ajili, M., Bonastre, J.-F., Ben Kheder, W., Rossato, S., Kahn, J. Dec. 2016. Phonetic content impact on Forensic Voice Comparison. *2016 IEEE Spoken Language Technology Workshop (SLT)* San Diego. IEEE p. 210–217.
- [2] Boersma, P. 2001. Praat, a system for doing phonetics by computer. *Glott International* 5:9/10, p. 341–345.
- [3] Galliano, S., Geoffrois, E., Mostefa, D., Bonastre, J.-F., Gravier, G. 2005. ESTER Phase II Evaluation Campaign for the Rich Transcription of French Broadcast News. *Proc. Interspeech* Lisboa, Portugal. p. 1149–1152.
- [4] Gendrot, C., Adda-Decker, M. 2005. Impact of duration on F1/F2 formant values of oral vowels: an automatic analysis of large broadcast news corpora in French and German. *Proc. Interspeech* Lisbon. p. 2453–2456.
- [5] Goodfellow, I., Bengio, Y., Courville, A. 2016. *Deep Learning*. Adaptive computation and machine learning. Cambridge, Massachusetts: The MIT Press.
- [6] Hershey, S., Chaudhuri, S., Ellis, D. P. W., Gemmeke, J. F., Jansen, A., Moore, C., Plakal, M., Platt, D., Saurous, R. A., Seybold, B., Slaney, M., Weiss, R., Wilson, K. 2017. CNN architectures for large-scale audio classification. *Proc. ICASSP* New Orleans. 131–135.
- [7] Hinton, G., Deng, L., Yu, D., Dahl, G. E., Mohamed, A.-r., Jaitly, N., Senior, A., Vanhoucke, V., Nguyen, P., Sainath, T. N., others, 2012. Deep neural networks for acoustic modeling in speech recognition: The shared views of four research groups. *IEEE Signal processing magazine* 29(6), 82–97.
- [8] Kingma, D. P., Ba, L. J. 2015. Adam: A Method for Stochastic Optimization. *International Conference on Learning Representations (ICLR)*. arXiv.org.
- [9] Koenig, W., Dunn, H. K., Lacy, L. Y. 1946. The Sound Spectrograph. *The Journal of the Acoustical Society of America* 18(1), p. 19–49.
- [10] Lozano-Diez, A., Plchot, O., Matejka, P., Gonzalez-Rodriguez, J. 2018. DNN based embeddings for language recognition. *Proc. of ICASSP* Calgary. p. 5184–5188.
- [11] Matějka, P., Glembek, O., Novotný, O., Plchot, O., Grézl, F., Burget, L., Cernocký, J. H. 2016. Analysis of dnn approaches to speaker identification. *Proc. ICASSP*. IEEE p. 5100–5104.
- [12] Morrison, G. S., Thompson, W., C. 2017. Assessing the admissibility of a new generation of forensic voice comparison testimony. *Columbia Science and Technology Law Review* 18, p. 326–434.
- [13] Nagamine, T., Seltzer, M. L., Mesgarani, N. 2015. Exploring how deep neural networks form phonemic categories. *Proc. Interspeech* Dresden. p. 1912–1916.
- [14] Nagrani, A., Chung, J. S., Zisserman, A. 2017. Voxceleb: a large-scale speaker identification dataset. *Proc. Interspeech* Stockholm.
- [15] Pellegrini, T. 2017. Densely connected CNNs for bird audio detection. *Proc. EUSIPCO* Kos. p. 1784–88.
- [16] Pellegrini, T., Mouysset, S. 2016. Inferring phonemic classes from CNN activation maps using clustering techniques. *Proc. Interspeech* San Francisco. p. 1290–1294.
- [17] Simonyan, K., Zisserman, A. 2015. Very Deep Convolutional Networks for Large-Scale Image Recognition. *ICLR 2015* San Diego.
- [18] Smith, J. O. accessed 13/11/2018. Spectral audio signal processing. <http://ccrma.stanford.edu/~jos/sasp/>. online book, 2011 edition.
- [19] Snyder, D., Garcia-Romero, D., Povey, D., Khudanpur, S. 2017. Deep neural network embeddings for text-independent speaker verification. *Proc. Interspeech* Stockholm. p. 999–1003.
- [20] Stevenage, S. V. July 2018. Drawing a distinction between familiar and unfamiliar voice processing: A review of neuropsychological, clinical and empirical findings. *Neuropsychologia* 116, 162–178.
- [21] Zeiler, M. D., Fergus, R. 2014. Visualizing and understanding convolutional networks. In: Fleet, D., Pajdla, T., Schiele, B., Tuytelaars, T., (eds), *Computer Vision – ECCV 2014* volume 8689. Springer p. 818–833.
- [22] Zhou, B., Khosla, A., Lapedriza, A., Oliva, A., Torralba, A. June 2016. Learning deep features for discriminative localization. *2016 IEEE Conference on Computer Vision and Pattern Recognition (CVPR)* Las Vegas. IEEE p. 2921–2929.